POLITECNICO DI TORINO
Repository ISTITUZIONALE

Air pollution and atmospheric variables in Türkiye: A comprehensive analysis

Original
Air pollution and atmospheric variables in Türkiye: A comprehensive analysis / Ciarlantini, S., Belis Claudio, A., Gavros, A., Pezzoli, A.. - In: ATMOSPHERIC POLLUTION RESEARCH. - ISSN 1309-1042. - (2025). [10.1016/j.apr.2025.102826]

Availability:
This version is available at: 11583/3005606 since: 2025-12-03T11:00:29Z

Publisher:
Elsevier

Published
DOI:10.1016/j.apr.2025.102826

Terms of use:

This article is made available under terms and conditions as specified in the corresponding bibliographic description in the repository

Publisher copyright

(Article begins on next page)

27 November 2026

Atmospheric Pollution Research xxx (xxxx) xxx

Contents lists available at ScienceDirect

Atmospheric Pollution Research

journal homepage: www.elsevier.com/locate/apr

Air pollution and atmospheric variables in Türkiye: A comprehensive analysis

Sara Ciarlantini [a,b,*,1], Claudio A. Belis [b], Andreas Gavros [c], Alessandro Pezzoli [a]

[a] Interuniversity Department of Regional and Urban Studies and Planning (DIST), Polytechnic of Turin and University of Turin, Turin, 10125, Italy
[b] European Commission, Joint Research Centre, Ispra, 21027, Italy
[c] Fincons SPA, Vimercate, 20871, Italy

ARTICLE INFO

Keywords:
Air quality
Atmospheric variables
Türkiye
Climatic regions
Particulate matter (PM_{10})
Sulphur dioxide (SO_2)
Generalised additive model (GAM)
Future scenarios

ABSTRACT

This study examines particulate matter (PM_{10}) and sulphur dioxide (SO_2) concentrations in Türkiye, one of the world's 20 largest economies with a population of more than 86 million people. The analysis covers from 2015 to 2019, a period during which pollutant levels frequently exceeded international air quality standards. While anthropogenic emissions are significant contributors, atmospheric variables also play a crucial role in pollutant dispersion and dilution. The research investigates how temperature, relative humidity, wind speed, precipitation, and boundary layer height affect pollutant concentrations in this country. Using a generalised additive model (GAM) and conducting a sensitivity analysis, the study explores seasonal and regional variations in the influence of these atmospheric variables across Türkiye, offering a national, multivariable perspective. The analysis relies on hourly data to capture diurnal variations during summer and winter. Additionally, it provides projections of pollutant concentrations for 2030 and 2050 under two IPCC climate scenarios: one assuming strong mitigation measures (RCP 4.5) and the other representing high-emission conditions (RCP 8.5). The GAM outputs show that temperature, humidity, wind speed, and precipitation affect PM_{10} and SO_2 differently across the country, with marked regional and seasonal variations. Winter PM_{10} commonly peaks near ~10 °C, whereas in several regions summer concentrations decline once temperatures exceed ~30 °C; relative humidity is generally positively associated with PM_{10} yet negatively with SO_2; stronger winds and precipitation coincide with lower pollutant levels (with PM_{10} highest at low winds <5 m/s and notably reduced on days with ~25 mm rainfall). Coastal regions show the strongest wind- and rain-related reductions in concentrations; interior continental and semi-arid regions display a weaker precipitation signal with a tighter humidity–PM_{10} association; and high-elevation basins and valleys are characterised by heightened sensitivity to boundary-layer stability. Sensitivity analysis indicates that boundary-layer height and wind are the primary atmospheric drivers for PM_{10}, whereas SO_2 shows a weaker overall sensitivity to atmospheric factors. Projections about the influence of atmospheric variables on pollution for 2030 and 2050 suggest that PM_{10} levels will generally decline across both seasons, while SO_2 concentrations are expected to rise during summer. The study highlights the increasing influence of climate change on air pollution, stressing the importance of region-specific air quality management strategies. By integrating mitigation and adaptation measures, the findings offer valuable insights for policymakers aiming to improve air quality and reduce health risks across Türkiye.

1. Introduction

With over 99 % of the world's population breathing unsafe air (UNEP, 2023), air pollution is one of the main environmental risks to public health (WHO, 2024). Over the recent decades, particulate matter and sulphur dioxide (hereafter referred to as PM and SO_2, respectively) originated from the burning of fossil fuels have emerged as the main components of air pollution in many parts of the world (WHO, 2021), and their harmful effects on health and the environment are widely documented (HEI, 2025; World Bank, 2022).

* Corresponding author. Interuniversity Department of Regional and Urban Studies and Planning (DIST), Polytechnic of Turin and University of Turin, Turin, 10125, Italy.
E-mail address: sara.ciarlantini@polito.it (S. Ciarlantini).
[1] Visiting Scientist at the European Commission, Joint Research Centre (JRC), Ispra, Italy.

https://doi.org/10.1016/j.apr.2025.102826
Received 20 May 2025; Received in revised form 9 November 2025; Accepted 11 November 2025
Available online 12 November 2025
1309-1042/© 2025 Turkish National Committee for Air Pollution Research and Control. Published by Elsevier B.V. This is an open access article under the CC BY license (http://creativecommons.org/licenses/by/4.0/).

Significant PM_{10} anthropogenic sources include industrial activities, construction processes (especially during earthwork and foundation stages; Yan et al., 2023), agricultural practices, and road transport. The latter also encompasses automobile exhaust emissions and tyre abrasion (Lenschow, 2001). Furthermore, natural sources, such as sea salt and desert dust, also contribute to the formation of PM_{10} (Ledoux et al., 2023). Within the group of sulphur oxide gases, SO_2 is the most prevalent in the atmosphere, and an increase in its concentrations leads to a higher risk of mortality (EPA, 2024). The largest source of SO_2 emissions in the atmosphere is fossil fuel combustion in power plants and other industrial facilities (EPA, 2024). Additionally, vehicles like locomotives, ships, and heavy equipment burning high sulphur content fuels contribute to these emissions. Natural sources, such as volcanoes, also play a role in releasing SO_2 into the atmosphere. The impact of these pollutants varies significantly across different geographical and socio-economic contexts, with rapidly developing economies often facing particularly serious challenges in managing air quality (HEI, 2025). These challenges typically arise from the complex interplay between rapid industrialisation, urbanisation, and existing environmental regulations (IQAir, 2024). Understanding these dynamics is crucial for developing effective air quality management strategies, especially in countries experiencing significant economic growth while striving to maintain environmental standards. This context is particularly relevant for understanding the air pollution challenges in Türkiye, where the combination of rapid economic development, geographic location, and complex atmospheric conditions creates a unique set of air quality management challenges.

Türkiye, with a population of more than 86 million people, is one of the world's 20 largest economies (FAO, 2024) and is affected by severe air pollution annual levels (European Commission, 2023). From 2009 to 2019, Türkiye continuously reported the highest (although decreasing) share of deaths attributed to air pollution compared to all EU-27 countries, with an average of 10 % of all-cause mortality (IHME - GHDx, 2019). According to The Right to Clean Air Platform, in this country air pollution is responsible each year for over 30,000 premature deaths due to stroke, ischemic heart disease, lung cancer, and chronic respiratory diseases (THPP. Right to Clean Air Platform, 2024).

Europe's air quality status in 2021 reveals that Eastern European countries, particularly Türkiye, reported SO_2 concentrations exceeding the EU daily limit value of 50 $\mu g/m^3$, and PM_{10} levels surpassing the EU daily limit of 45 $\mu g/m^3$—both established by Directive (EU) 2024/2881 and set to be enforced in 2030 (European Parliament and Council, 2024)—as well as the WHO daily guideline of 45 $\mu g/m^3$ (EEA, 2023). In 2017, only 1 out of 81 Turkish cities had PM_{10} levels below the WHO guideline levels (THPP. Right to Clean Air Platform, 2024). Notably, in this country, daily average PM_{10} levels often exceed 75 $\mu g/m^3$, with concentrations generally stable, except in specific provinces like Edirne and Kahramanmaraş, where air pollution has become a prominent issue (Aykaç and Yasin, 2021).

Episodes of high concentrations of air pollutants in urban and sub-urban areas are not exclusively caused by abrupt rises in emissions, but atmospheric conditions significantly control the dispersion and the accumulation of pollutants, as well as favour their formation through chemical reactions (e.g. photochemical formation of ozone; Han et al., 2015; Latini et al., 2002; Ma et al., 2021; Qi et al., 2021). Atmospheric variables impacting air quality fall into two main categories (Latini et al., 2002): (a) variables that, through mechanical dispersion, influence the accumulation and spatial distribution of pollutants, such as atmospheric stability, temperature, wind, precipitation, and relative humidity; and (b) variables that impact the chemical transformations of pollutants, varying depending on the type of pollutant. Rather than focusing on the role of a single atmospheric parameter in the accumulation and dispersion of air pollutants, it is essential to examine multiple atmospheric variables collectively, as their interplay has the most significant impact on air pollutant concentrations (Qi et al., 2021; Van Nieuwenhuyse et al., 2023). To do so, most analytical methods have traditionally relied on linear approaches (Ravindra et al., 2019), despite evidence that nonlinear statistical methods can more effectively capture the complex relationships between meteorological variables and air pollution (Thompson, 2001).

This study moves beyond traditional single-variable approaches by applying a harmonised, multivariable generalised additive model (GAM) framework to recent air-quality data across Türkiye. Prior research has typically focused on individual cities (e.g. Çelik and Kadi, 2007; İçağa and Sabah, 2009; Ulutaş et al., 2021) and on one or two atmospheric variables rather than a broader set of potentially influential atmospheric drivers (İçağa and Sabah, 2009; Tasdemir et al., 2005; Ulutaş et al., 2021); a national, multivariable perspective therefore offers a more comprehensive view of how atmospheric conditions may shape pollutant concentrations. Moreover, much of the existing literature relies on observations from the late 1990s and early 2000s, underscoring the need for updated datasets (Cuhadaroglu and Demirci, 1997; Kartal and Özer, 1998; Tayanç et al., 1997).

For all the mentioned reasons, this study aims to: (i) analyse recent (since 2015) air pollutant concentration time series across Türkiye, assessing the combined influence of different atmospheric variables on PM_{10} and SO_2 levels, and examining regional differences in air quality using a GAM combined with a sensitivity analysis framework; and (ii) evaluate how future climatic conditions may affect pollutant concentrations in 2030 and 2050, assuming all other variables remain constant, under two contrasting climate scenarios—one reflecting strong mitigation efforts and the other representing an extreme case. The innovative strength of this research lies in combining multiple analytical techniques to capture the dynamics of air pollution in relation to historical trends and projected climatic scenarios, though the use of a nonlinear statistical approach.

2. Methodology

2.1. Data resources

Hourly concentrations of PM_{10} ($\mu g/m^3$) and SO_2 ($\mu g/m^3$) are obtained from the European Environment Agency platform (EEA, 2024). These two pollutants are selected because they provide the most complete temporal and spatial coverage across national monitoring stations, as they serve as suitable indicators for assessing meteorological influences on air quality, whereas other pollutants, such as NO_2, are less responsive to meteorological variability (EEA, 2025). Background stations are chosen as they can capture integrated contributions from various sources while excluding traffic and industrial stations (DEFRAUK Air, 2023). The final selection includes 42 air quality monitoring stations, located in urban, suburban, and rural areas.

To examine the impact of climate on air pollution levels, in-situ meteorological stations located within 5 km of the nearest air quality monitoring station are selected to ensure consistency across sites (Colston et al., 2018). This approach ensures paired hourly meteorology for each air-quality station, overcoming slight differences in air pollution data caused by the geographical distribution of monitoring stations (Hou and Xu, 2022). The National Oceanic and Atmospheric Administration database (NOAA, 2024) provides hourly observations of: (a) temperature (°C), (b) wind speed (m/s), (c) wind direction (degree), (d) sea level pressure (hPa). Through an elaboration of these variables, the following ones are also calculated: (e) relative pressure (measured against the average atmospheric pressure of the preceding 30 years; hPa), and (f) relative humidity (calculated from air and dewpoint temperatures measurements; %). Hourly data observations of total precipitation (mm) and boundary layer height (hereafter BLH; m) are unavailable from the NOAA database. Thus, they are retrieved from the outputs of ERA5 (Hersbach et al., 2020), i.e. the fifth generation reanalysis produced by the European Centre for Medium-Range Weather Forecasts (ECMWF, 2024). Combining past observations with models, ERA5 outputs are produced hourly at a horizontal resolution of 31 km.

The total number of meteorological stations is 39, as three different air quality monitoring stations (namely Alsancak, Bayrakli, and Sirinyer) share a common NOAA station within 5 km.

The selection of monitoring stations follows a rigorous multi-step process to ensure data quality and representativeness: (i) continuous coverage for consecutive years; (ii) ≥75 % annual completeness; and (iii) spatial representativeness across all Türkiye's climatic regions. Although a five-year window is shorter compared to some climatological studies, several factors support the validity and relevance of our results: (i) the high temporal resolution (hourly measurements) enables detailed analyses of diurnal and seasonal cycles and their relationships with atmospheric variables; and (ii) the broad spatial coverage, with stations distributed across all Turkey's seven climatic regions, provides geographical robustness.

Data for future climate projections are obtained from the Copernicus Climate Data Store (Copernicus, 2024). The dataset provides daily projections of temperature, relative humidity, precipitation, and wind speed for the years 2030 and 2050 at a 25 km resolution (see Supplementary section – Part 1a). These variables are selected under two different future Intergovernmental Panel on Climate Change (IPCC) scenarios, based on Representative Concentration Pathways (RCPs): RCP 4.5 and RCP 8.5. Future yearly mean concentrations are derived from the hourly data of pollutants and atmospheric variables, following a similar approach to Çapraz et al. (2016).

2.2. Study area

The location of the 42 air quality monitoring stations and 39 meteorological stations is shown in Fig. 1. More information about the stations (e.g. coordinates, elevation, distance) can be found in Table S1 in the Supplementary content.

Türkiye has been conventionally divided into seven climatic zones (Erinç, 1984 in Sahin and Kerem Cigizoglu, 2012): (1) Marmara, around the Sea of Marmara bordering Greece and Bulgaria; (2) Aegean, on the west coast; (3) Mediterranean, Türkiye's southern shore; (4) Black Sea, Türkiye's Black Sea coast; (5) Central Anatolia, the vast inland plateau in the centre; (6) Eastern Anatolia, at east adjacent to Iran and the Caucasus countries; and (7) Southeastern Anatolia, bordering Syria and Iraq. These seven climatic regions are shown in Fig. 2. The climate of Türkiye is heavily influenced by its physiographic features, such as mountain chains and surrounding seas, with the latter acting as natural passages for frontal cyclones moving from west to east (Türkeş, 1996). Large-scale atmospheric circulation patterns also play a crucial role in shaping Türkiye's atmospheric conditions (Deniz et al., 2011). During winter, the influence of the polar front and cold air masses from the Balkans is associated with frontal passages and lower temperatures. In contrast, the polar front shifts northward during summer, leading to weaker frontal passages and increased maritime influences. Anticyclonic pressure patterns, such as the Azores high-pressure system in summer and the Siberian anticyclone in winter, further impact Türkiye's climate dynamics.

2.3. Study design

2.3.1. Missing data management

A conservative approach is adopted regarding missing data: results are based solely on observed data, avoiding imputation techniques to prevent the introduction of potential biases (Alwateer et al., 2024; Donders et al., 2006). Instead, we focused on the careful selection of stations with high data completeness, ensuring the integrity of the analysis.

The missing data analysis reveals slightly different patterns across stations and variables. For air quality data, the percentage of missing values over the 5-year period ranged from 0.77 % to 15 %, depending on the station, with average missing rates of 4.45 % for PM_{10} and 3.3 % for SO_2. For atmospheric variables, data completeness is generally higher than for air quality data. Precipitation and BLH are 100 % complete across all stations, while temperature, relative humidity, and wind speed have occasional missing values, with the highest percentage reaching 1.15 % at some stations. A detailed overview of missing data for each station and variable can be found in Table S2 of the Supplementary content.

Temporal analysis of missing data reveals no clear seasonality or trends, indicating that data are missing completely at random (MCAR),

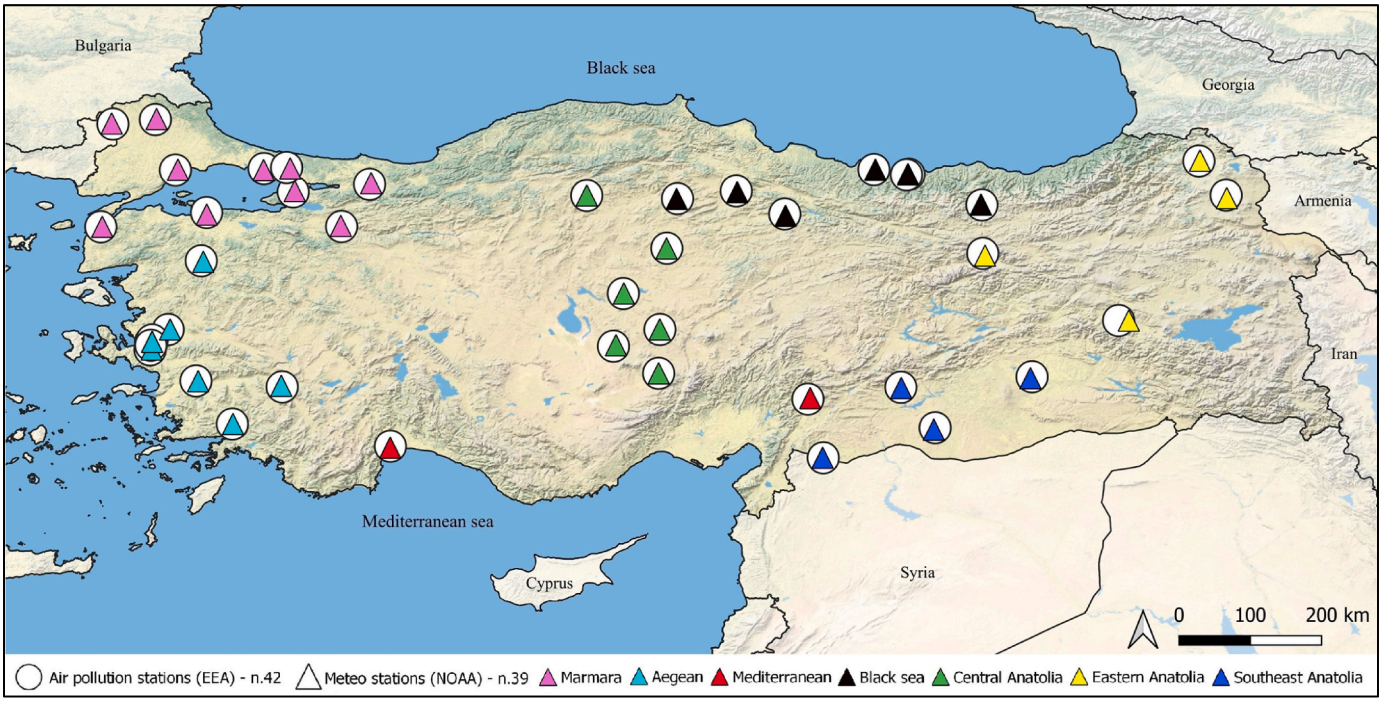

Fig. 1. Elevation map of the study area with the location of the 42 air quality monitoring stations (white circles) and the 39 meteorological stations (triangles coloured according to the climatic region of belonging) across Türkiye.

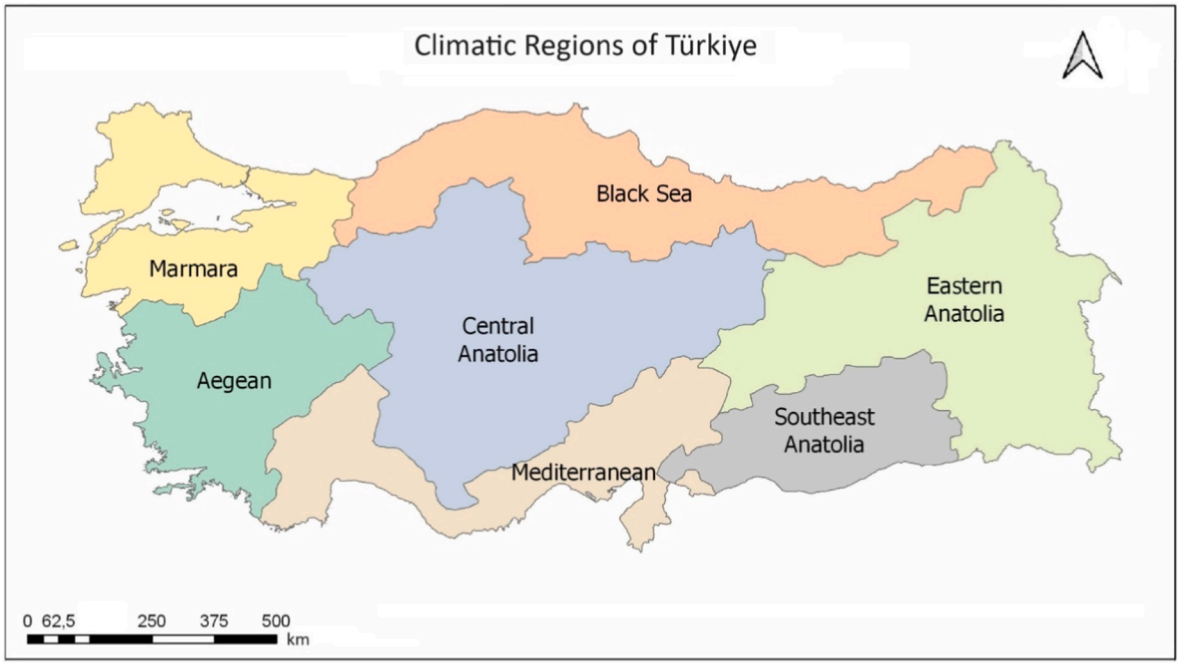

Fig. 2. Türkiye's seven climatic regions (figure adapted from Mappr, mappr.co).

rather than being influenced by environmental or operational factors (Little, 1988). In the few cases where data are missing, logistic regression analyses could not be performed due to the rarity of missing values, reinforcing the assumption of randomness.

2.3.2. Climate normals

To ensure that the climate data in the analysis aligns with the long-term climate, it is necessary to compare the 2015–2019 statistics with the climatological normal, i.e. the monthly averages computed for a prolonged period of at least 30 consecutive years. Such comparison helps verify that there have not been significant changes in the climate over time (WMO, 2017) and ensures that the years used in the analysis are not "exceptional" (for example, extremely cold or warm) compared to the "normal" climate.

This study uses the 30-year 1985–2014 period to calculate the temperature, sea level pressure, and relative humidity climate normals, following the World Meteorological Organization guidelines (WMO, 2017). Despite some discrepancies between the 2015–2019 and the 1985–2014 distributions, also considering the rise in temperature over recent decades, such differences are statistically insignificant, meaning that the data of this study for the limited 5-year period is not unusual or drawn from exceptional atmospheric conditions (according to the Kolmogorov-Smirnov, Mann-Whitney U and Kruskal-Wallis statistical tests - Berger and Zhou, 2014; MacFarland and Yates, 2016; McKight and Najab, 2010; see Fig. S3).

2.3.3. Statistical measures for comparison

This study applies GAMs to better capture how atmospheric variables influence air pollution patterns at a national scale. GAMs are an extension of traditional regression models, where smoothing splines replace linear coefficients for covariates (Hastie, 2017). They provide a more flexible and effective framework than conventional linear models for analysing relationships between air pollutants and atmospheric variables, which are often nonlinear and not normally distributed (Pearce et al., 2011; Thompson, 2001). The GAM analyses are conducted separately for winter and summer in each of Türkiye's climatic regions, with seasonal classification based on a 24-month dataset corresponding to northern hemisphere seasons. Additional details on the GAM methodology, including equations and references, are provided in the Supplementary section (Part 1b).

The GAM approach adopted in this study offers advantages in terms of data-driven analysis, ability to capture nonlinear relationships, and direct interpretation of complex atmospheric-pollution associations from observational data. This statistical methodology has been successfully applied in numerous air quality studies (Thompson, 2001; Pearce et al., 2011; Hou and Xu, 2022), providing a robust framework for analysing complex environmental relationships, while acknowledging that it represents these relationships statistically rather than mechanistically.

A sensitivity analysis is also conducted to evaluate variables' contribution to uncertainty of the predicted PM_{10} and SO_2 concentrations. The adopted SIMLAB software (Joint Research Centre, 2024) employs moment-independent sensitivity indices derived from both the probability density function method (Plischke et al., 2013) and the cumulative density function method (Pianosi and Wagener, 2015). The former examines how the complete probability distribution of the model outputs changes in response to variations in input parameters, while the latter focuses on the accumulated effects of parameter variations across their entire range of values. The resulting sensitivity indices quantify the relative contribution of each atmospheric variable to the model's uncertainty, providing crucial information for understanding which parameters most strongly influence pollutant concentrations in different regions and seasons.

2.3.4. Model selection and validation

In this study, two models are tested: a linear model and a GAM. Both models use PM_{10} or SO_2 concentrations as the response variable (Y) and four atmospheric variables (temperature, relative humidity, wind speed, and precipitation) as predictors (X).

The comparative evaluation of the models is conducted through four quantitative performance metrics: (i) explained deviance measures the proportion of variability in the data captured by the model (Hastie, 2017); (ii) the Akaike Information Criterion (AIC) assesses the balance between goodness of fit and model complexity, with lower values indicating better models (Akaike, 1974); (iii) Root Mean Square Error (RMSE) and (iv) Mean Absolute Error (MAE) quantify the average magnitude of prediction errors, where smaller values represent better predictive performance (Chai and Draxler, 2014).

3. Results and discussion

3.1. Air quality seasonal trends

To analyse the seasonal differences in air pollutant concentrations, the seasonal cycles of both PM_{10} and SO_2 are plotted in Fig. 3. For both pollutants, higher concentrations are recorded during colder months (from November to February) compared to warmer months (from May to August). This seasonal pattern aligns with those observed for PM_{10} in 81 Turkish cities (Kabatas et al., 2014), SO_2 in 50 Turkish sites (Bozkurt et al., 2018), and both pollutants in 75 Turkish city centres (Güneş, 2005). High levels of PM_{10} during winter are expected due to significant local and regional pollution sources (Kabatas et al., 2014). The atmospheric conditions in winter, such as lower BLH, do not favour the dispersion of pollutants, leading to elevated PM_{10} levels. In contrast, PM_{10} concentrations are generally lower during warm seasons, reflecting the reduced pollution sources and more favourable atmospheric conditions for dispersion. Additionally, during the transition seasons, particularly spring and autumn, Saharan dust outbreaks can contribute to spikes in PM_{10} levels (Kabatas et al., 2018). These dust events, originating from the Sahara desert, may impact air quality in Türkiye, explaining the occasional high PM_{10} measurements even during typically lower-pollution seasons. Similarly, SO_2 levels follow a seasonal trend, with higher concentrations observed in winter compared to other seasons (Bozkurt et al., 2018). This increase primarily corresponds to the widespread use of coal and other fossil fuels for heating, greater traffic intensity, and atmospheric conditions like reduced mixing height, as described above.

Fig. 4 illustrates the spatial variability of mean PM_{10} (a–b) and SO_2 (c–d) concentrations across Türkiye during winter and summer, aggregated over the period 2015–2019.

For PM_{10}, concentrations during winter reach up to 100 $\mu g/m^3$ (Fig. 4a), whereas in summer they generally remain below 25 $\mu g/m^3$, with mean values not exceeding 75 $\mu g/m^3$ (Fig. 4b). Higher PM_{10} seasonal levels are observed in the Marmara, Aegean, and Eastern Anatolia regions compared to other regions, while the Black Sea region records lower concentrations. This latter pattern likely reflects the area's consistent year-round precipitation, which contributes to improved air quality (Sensoy and Demircan, 2016; see Fig. 2 for climatic region divisions).

SO_2 concentrations exhibit a marked seasonal contrast (Fig. 4c and d). In winter, elevated levels are observed across all regions, with averages exceeding 50 $\mu g/m^3$ in the Marmara, Aegean, and Central Anatolia regions (Fig. 4c). During summer, mean SO_2 concentrations drop to 10 $\mu g/m^3$ (or lower) at most stations (Fig. 4d). Notable exceptions include Muğla, in the Aegean region—likely due to emissions from three coal-fired power plants located in the area—and Ardahan, in Eastern Anatolia, where low temperatures and socio-economic variables contribute to reliance on inexpensive, low-calorific coal with high sulphur content (Demir et al., 2014).

Overall, the Marmara and Aegean regions are identified as highly polluted for both PM_{10} and SO_2. Compared to other regions, Eastern Anatolia experiences relatively higher PM_{10} concentrations, while Central Anatolia shows higher SO_2 levels.

3.2. Atmospheric variables trends

The mean seasonal cycles of temperature, relative humidity, wind speed, and precipitation from the monitoring stations are presented in Fig. 5. As expected, considerable climatic differences emerge among the seven regions of the country. Eastern Anatolia stands out as the coldest region year-round, with average minimum temperatures frequently falling below 0 °C, with the highest average monthly temperature of 23.5 °C in August. At the other extreme, Southeast Anatolia records the highest average temperatures in Türkiye, especially during summer. In this season, mean temperatures regularly exceed those of the Mediterranean region (Türkiye's second hottest area) by several degrees Celsius. This highlights Southeast Anatolia's distinctly arid and hot summer conditions. Coastal regions such as the Mediterranean and Aegean also experience high summer temperatures, though moderated by their proximity to the sea.

In terms of humidity, the Black Sea region displays a distinctly moist climate. It is the only region in Türkiye that receives consistent precipitation year-round (Sensoy and Demircan, 2016), maintaining relative humidity levels above 50 % in all seasons. In contrast, Southeast Anatolia experiences the lowest relative humidity levels, particularly in summer, when values drop below 30 % due to its arid conditions and high temperatures. The Marmara region maintains the highest relative humidity levels throughout the year, consistently above 60 %.

Wind speed patterns show distinct seasonal cycles. The strongest winds are recorded in summer, driven by significant temperature differences between land and sea (Şahin and Türkeş, 2013). Conversely, autumn sees the weakest winds as temperature gradients and pressure differences diminish following the end of summer. The highest wind

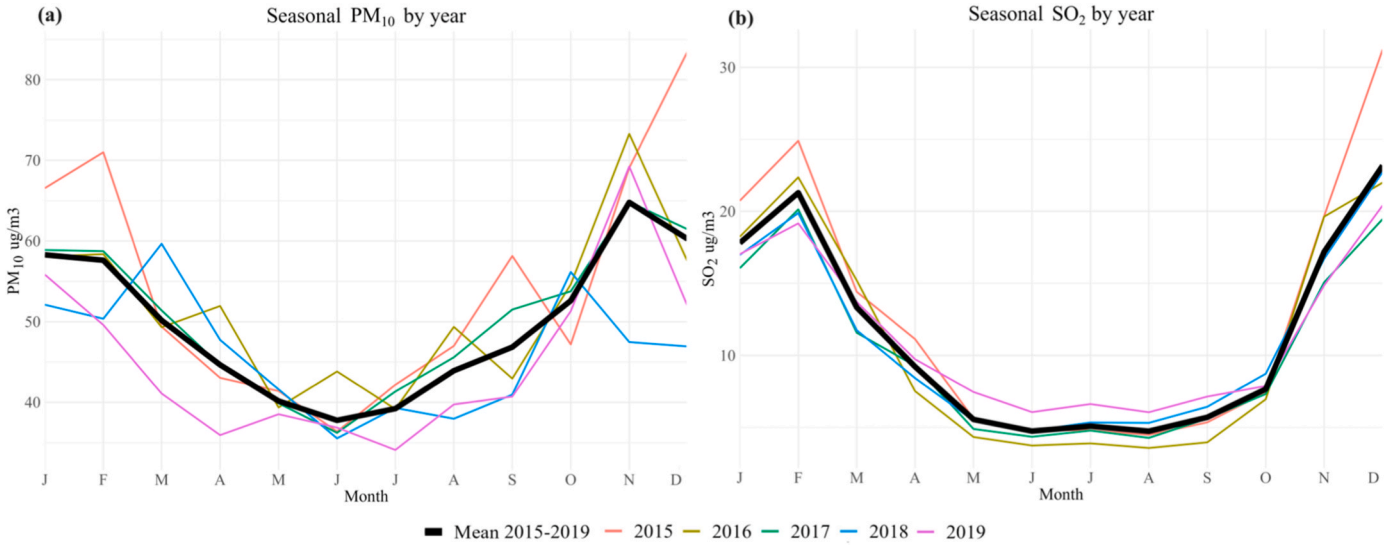

Fig. 3. Mean (i.e. averaged over all 42 monitoring stations) seasonal cycle of PM_{10} (a) and SO_2 (b) concentrations for 2015–2019 (black line) and each year of the 2015–2019 period (coloured lines).

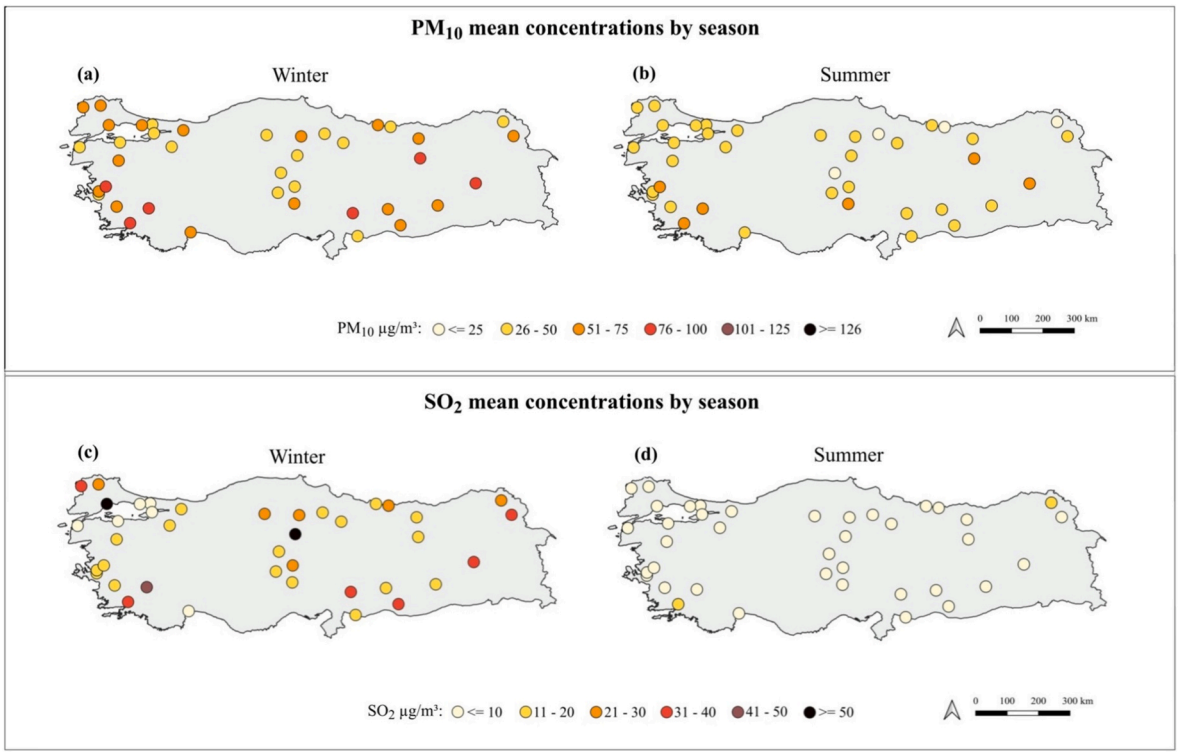

Fig. 4. Spatial distribution of the seasonal mean concentrations of observed PM_{10} for winter (a) and summer (b), and SO_2 for winter (c) and summer (d), across 42 monitoring stations during the period 2015–2019.

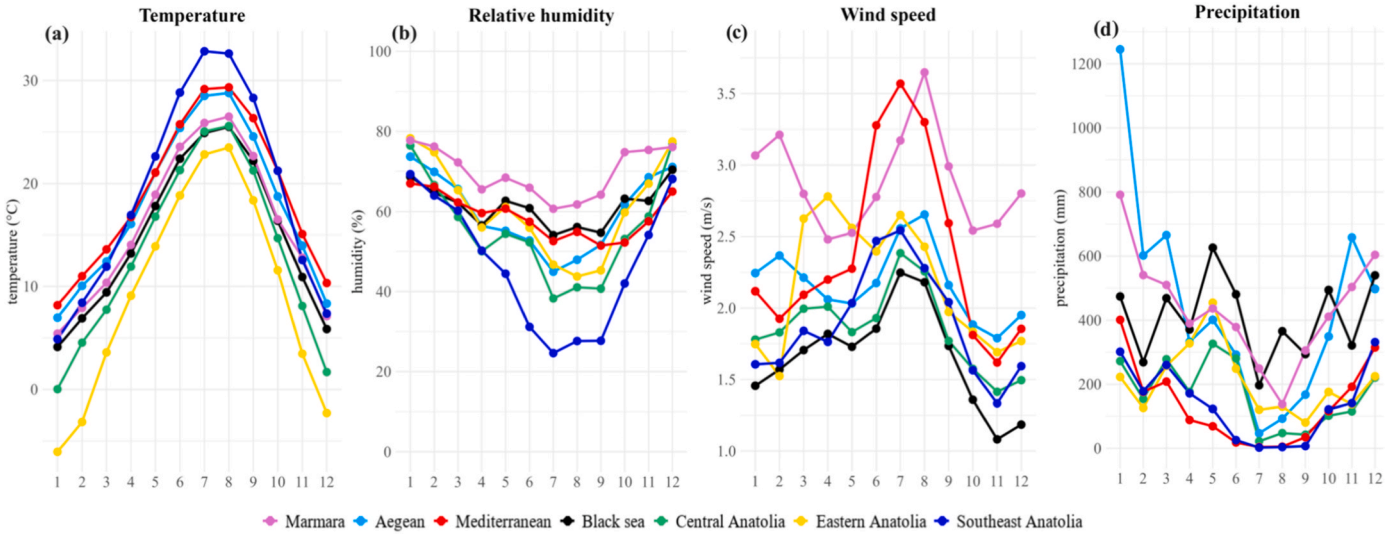

Fig. 5. Mean seasonal cycle of temperature (a), relative humidity (b), wind speed (c) and precipitation (d) for each climatic region of Türkiye during 2015–2019.

speeds occur in coastal regions, particularly in the Aegean and Mediterranean areas. In the Aegean region, strong summer winds are largely due to the Etesian winds—persistent northerly flows that prevail over the Aegean Sea during summer and early autumn (Şahin and Türkeş, 2020).

Precipitation patterns also vary significantly. Eastern and Central Anatolia, the second coldest region, receive low precipitation throughout the year due to the blocking effects of the South and North Anatolian mountain chains, which run parallel to the Mediterranean and Black Sea coasts, respectively (Deniz et al., 2011). Conversely, the Black Sea region again stands out as the wettest area, while the coastal regions—Marmara, Aegean and Mediterranean—experience wetter winters and hot, dry summers. These dry summer conditions are often associated with persistent anticyclonic systems over the central and eastern Mediterranean Basin (Türkeş, 1996).

3.3. Impact of atmospheric variables on air quality

Changes in pollutants levels are influenced not only by seasonal meteorological variations but also by other atmospheric variables (Kayes et al., 2019; Manju et al., 2018). This section examines how such variables influence pollutant concentrations during winter and summer, which represent the periods of highest and lowest levels, respectively, for the two studied pollutants (Figs. 3 and 4) using GAM, as it

consistently outperforms the linear model across all metrics and climate regions (see Supplementary section – Part 1c).

For both seasons and across each of Türkiye's seven climatic regions, the dependencies of PM_{10} and SO_2 on temperature, relative humidity, wind speed, and precipitation are illustrated in Fig. 6 for PM_{10} and Fig. 7 for SO_2. It is important to note that these atmospheric variables are naturally interdependent; for example, temperature and relative humidity often vary together. This correlation among predictors complicates the attribution of effects to individual variables, as their influences on pollutant concentrations may not be entirely separable. However, the analysis of these interdependencies is beyond the scope of this study. Moreover, it should be noted that the model assumes that stations within the same climatic region share similar characteristics, which may not account for local topographical or microclimatic variations. Furthermore, the uneven spatial distribution of monitoring stations, particularly in rural and complex terrain areas, limits the model's ability to provide comprehensive coverage.

The GAM outputs reveal a complex interplay between **temperature** and PM_{10} concentrations across Turkish regions. In winter, PM_{10} levels typically peak around 10 °C, yet the subsequent trend differs by region: while concentrations decline with increasing temperature in the Aegean, Marmara, and Mediterranean regions, they continue to rise in the Black Sea, Eastern Anatolia, and Southeast Anatolia. While our dataset includes only surface measurements and does not contain direct observations of vertical temperature profiles, previous studies have shown that low surface temperatures and high atmospheric pressure in winter are often correlated with conditions favourable for thermal inversions (Feng et al., 2020). Under such conditions, vertical air mixing can be reduced, potentially contributing to higher pollutant concentrations near the ground. However, we emphasise that our statistical associations do not demonstrate the actual presence of inversion layers. During summer, a generally weak positive temperature dependency is observed, yet in the Black Sea, Eastern Anatolia, and Southeast Anatolia, PM_{10} levels begin to drop when temperatures exceed 30 °C. In contrast, SO_2 exhibits a predominantly negative relationship with temperature in both seasons (except in the Black Sea and Southeast Anatolia, where the patterns become more complex with temperature variations). This may be because high temperatures could enhance the instability of SO_2 (Hou and Xu, 2022). It is important to note that the temperature measurements used in this study represent surface-level observations at individual meteorological stations and not vertical temperature profiles. While our analysis identifies statistical associations between these surface measurements and pollutant concentrations, we cannot directly observe atmospheric thermal stratification or boundary layer dynamics from these data alone.

Relative **humidity** also plays a significant role in modulating pollutant levels. In winter, most regions show a positive correlation between PM_{10} concentrations and relative humidity, meaning higher humidity coincides with increased pollutant levels—Central Anatolia being the only exception, where higher humidity is associated with lower concentrations. A similar pattern emerges in summer, with the majority of regions exhibiting positive dependencies between PM_{10} and humidity; however, in Central Anatolia the dependence remains negative, while in the Black Sea region PM_{10} levels initially decrease at relative humidity levels below 40 % before stabilising. Unlike PM_{10}, SO_2 generally maintains a negative dependency on relative humidity in both winter (albeit moderately) and summer (particularly pronounced in the Aegean and Marmara). Our analysis reveals a significant association between increased relative humidity and decreased SO_2 concentrations. While this pattern is consistent with the physical process of SO_2 dissolution in water droplets described by Hou and Xu (2022), our statistical approach cannot confirm this as the actual mechanism. Other factors that covary with humidity might also contribute to the observed pattern. Exceptions include the Mediterranean region in winter, where an overall positive correlation is observed, and Southeast Anatolia in summer, where a clear positive relationship emerges, as well as the Black Sea region, where a moderate positive dependency is noted.

Wind speed emerges as another key factor, inversely associated with PM_{10} concentrations, with relationships observed between wind patterns and dispersion through turbulence and horizontal transport. This relationship is particularly pronounced during winter, notably in coastal areas—such as the Aegean, Marmara, Mediterranean, and Black Sea—where higher wind speeds correlate with notable reductions in PM_{10}. Wind speed is also linked to SO_2 dispersion patterns, particularly in winter, where negative dependencies are observed across most regions. In the Aegean and Marmara, SO_2 concentrations peak at low wind speeds (1 m/s and 2 m/s, respectively) before declining as wind speed increases. Moreover, station-level polar plot analyses indicate that periods of low wind speed (<5 m/s), with high frequencies close to the origin, are associated with the highest pollution levels (see Fig. S4). Additionally, analysis of the BLH suggests a statistical relationship between BLH values and pollutant concentrations (see Fig. S5). However, it is important to note that these reanalysis-derived BLH values represent model outputs that incorporate multiple atmospheric variables and should not be interpreted as direct observations of atmospheric mixing processes. The statistical associations observed between BLH and pollutant concentrations should be considered as indications of potential relationships rather than demonstrations of physical causal mechanisms. This pattern is especially noticeable in valleys, where downslope cold air flow appears connected to boundary layer stability. Overall, the GAM results indicate that PM_{10} shows stronger statistical relationships with wind-driven dispersion than SO_2. This difference may be associated with the relative proximity of PM_{10} sources to monitoring stations, in contrast to SO_2 sources, such as power plants, which are typically more distant.

Precipitation further shows relationships with pollutant dynamics through wet deposition processes. In winter, a strong negative dependency is evident for PM_{10}, especially in regions like the Mediterranean where daily rainfall can reach 25 mm; here, higher rainfall corresponds to lower PM_{10} levels. Southeast Anatolia, however, displays a relatively flat relationship, potentially connected to its arid climate and the region's limited rainfall. In summer, when rainfall is generally lower across all regions compared to winter, this dependency weakens. Nonetheless, PM_{10} concentrations still peak under very low precipitation and decline as rainfall increases, although less markedly than in winter. The relationship between precipitation and SO_2 concentrations remains weakly negative in both seasons, with regions such as Southeast Anatolia displaying little to no dependency. Overall, these patterns are consistent with a correlation between wet deposition—through mechanical washout for PM_{10} and chemical dissolution and subsequent oxidation for SO_2—and reduced atmospheric pollutant levels.

The sensitivity analysis quantifies the importance of each atmospheric variable, reinforcing our findings and highlighting the key contributors to the model's uncertainty. For PM_{10} in winter, BLH consistently shows the highest sensitivity indices across all stations, indicating its statistical association with pollutant dispersion and vertical mixing patterns. In most regions, precipitation is the second most influential factor, followed by wind speed. Notably, in the Aegean, Marmara, and Southeast Anatolia regions, wind speed emerges as more influential than precipitation. Greater regional variation emerges in summer: wind speed is the primary driver in coastal areas, temperature in the Black Sea and Eastern Anatolia regions, and precipitation in Central and Southeast Anatolia. For SO_2 concentrations, atmospheric variables contribute less—or not at all—to the model's uncertainty compared to PM_{10}. In winter, wind speed is the predominant factor in most regions, except in Eastern Anatolia and the Mediterranean, where temperature is more influential, and in Southeast Anatolia, where relative humidity plays a larger role. In summer, precipitation is generally the most influential variable, except in the Black Sea and Eastern Anatolia regions, where relative humidity has the greatest impact.

The statistical relationships identified in this study should be interpreted with consideration of several potential confounding factors that

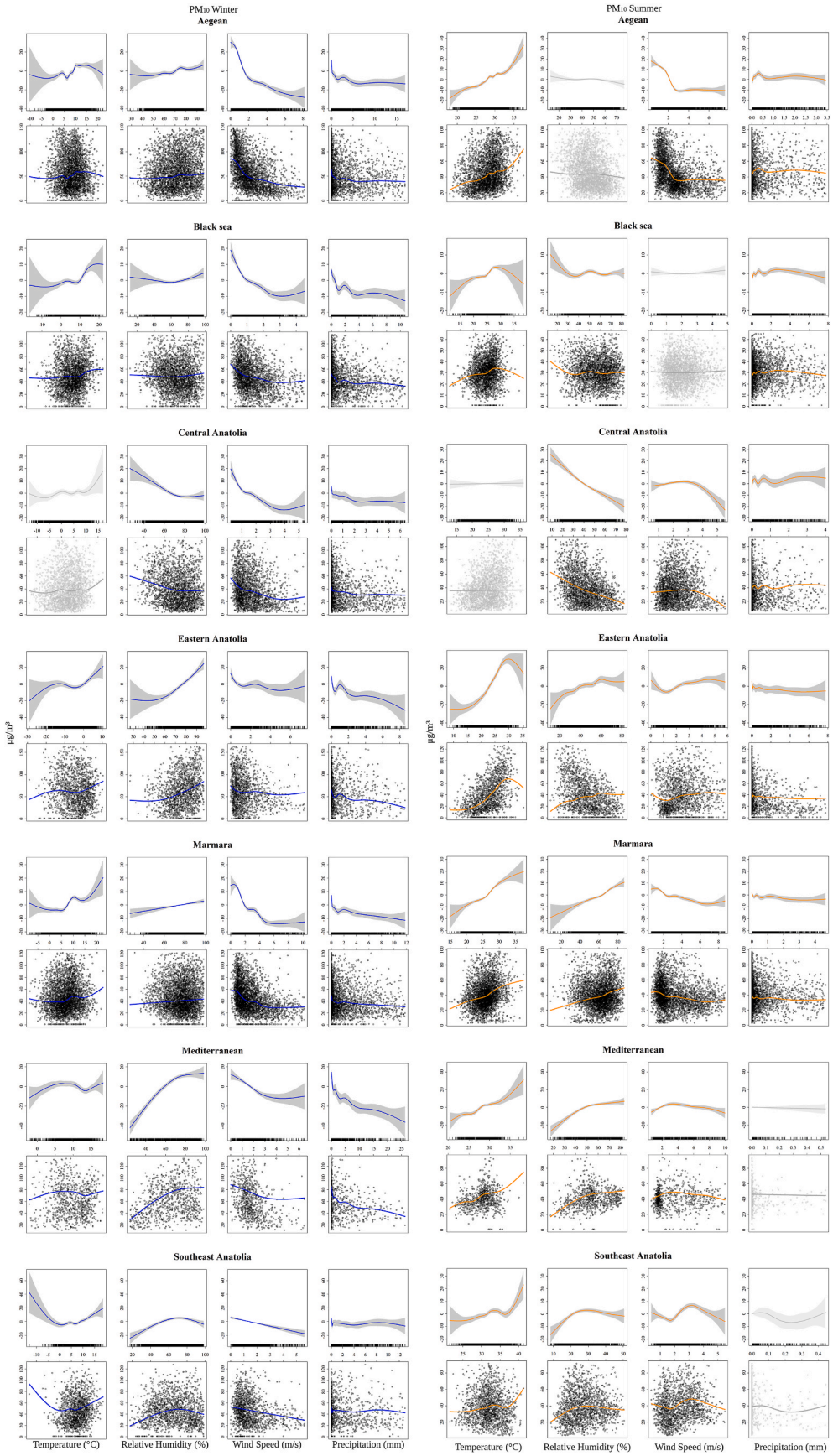

Fig. 6. PM_{10} GAM outputs for each of the 7 climatic regions in winter and summer. Each figure presents two panels: 1) The upper panel shows the estimated smoother for each variable derived from the GAMs (Y-axis); 2) The lower panel displays the corresponding fitted values (Y-axis). To calculate the fitted values, the estimated smoother was combined with the model's intercept (Zuur, 2012).

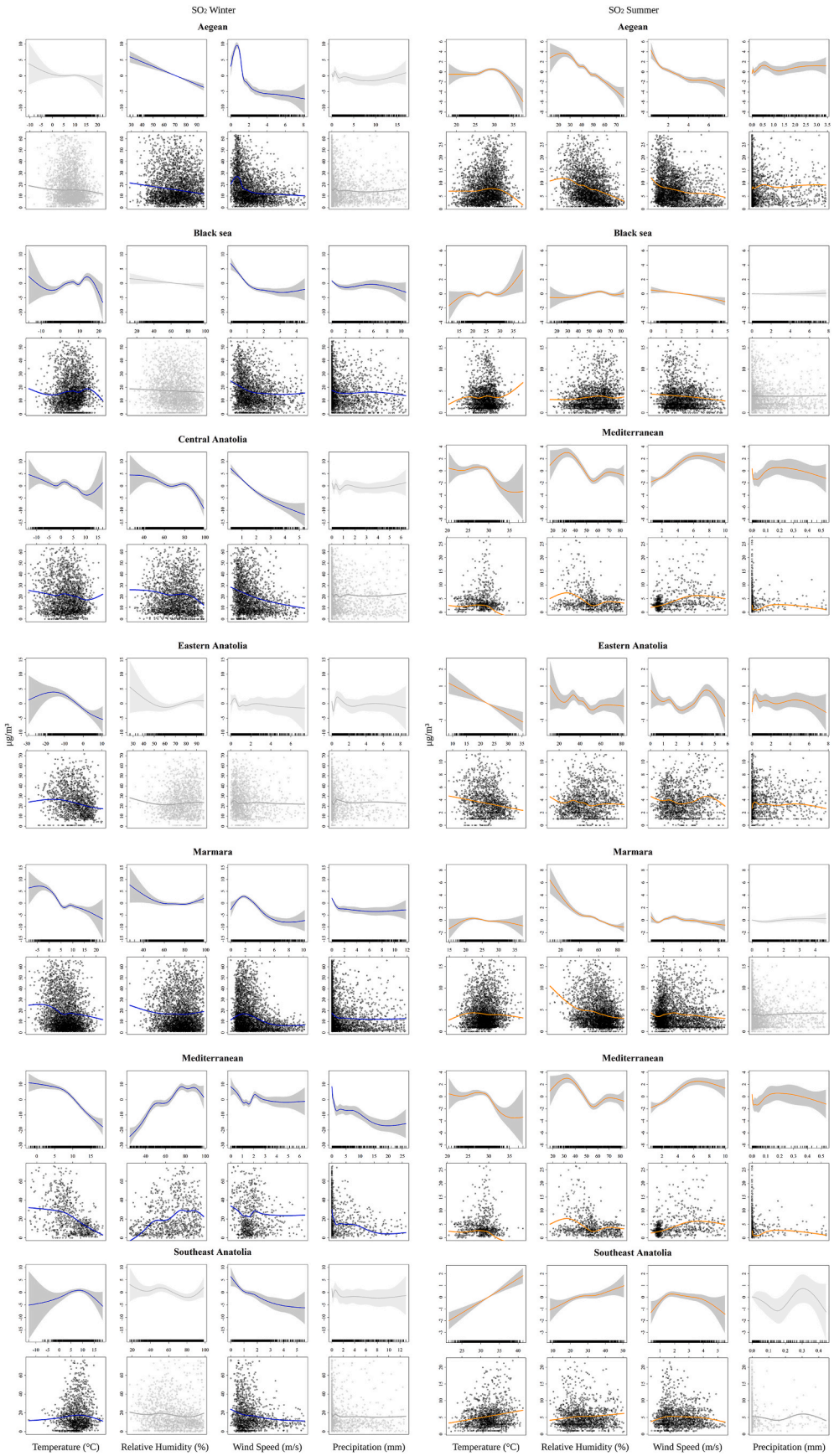

Fig. 7. SO_2 GAM outputs for each of the 7 climatic regions in winter and summer. Each figure presents two panels: 1) The upper panel shows the estimated smoother for each variable derived from the GAMs (Y-axis); 2) The lower panel displays the corresponding fitted values (Y-axis). To calculate the fitted values, the estimated smoother was combined with the model's intercept (Zuur, 2012).

are not explicitly included in our model. These include:

- Seasonal variations in emissions from heating, transportation, and industrial activities that may covary with meteorological conditions
- Land use patterns and topographical features that influence both local climate and pollution dispersion
- Regional and transboundary pollution transport patterns
- Changes in energy consumption behaviour that may correlate with temperature and other weather conditions
- Policy interventions and regulatory activities during the study period

These factors may create apparent statistical associations between atmospheric variables and pollutant concentrations that do not reflect direct physical relationships. While our statistical approach helps identify patterns, it cannot fully disentangle these complex interactions.

Furthermore, even the relationships identified should be interpreted within the context of atmospheric system complexity. For example, the apparent relationship between wind speed and pollutant concentrations represents a statistical association that simplifies numerous underlying processes, including turbulent mixing, horizontal transport, and the interaction between local and synoptic meteorological conditions. Similarly, temperature-pollution relationships may reflect not only

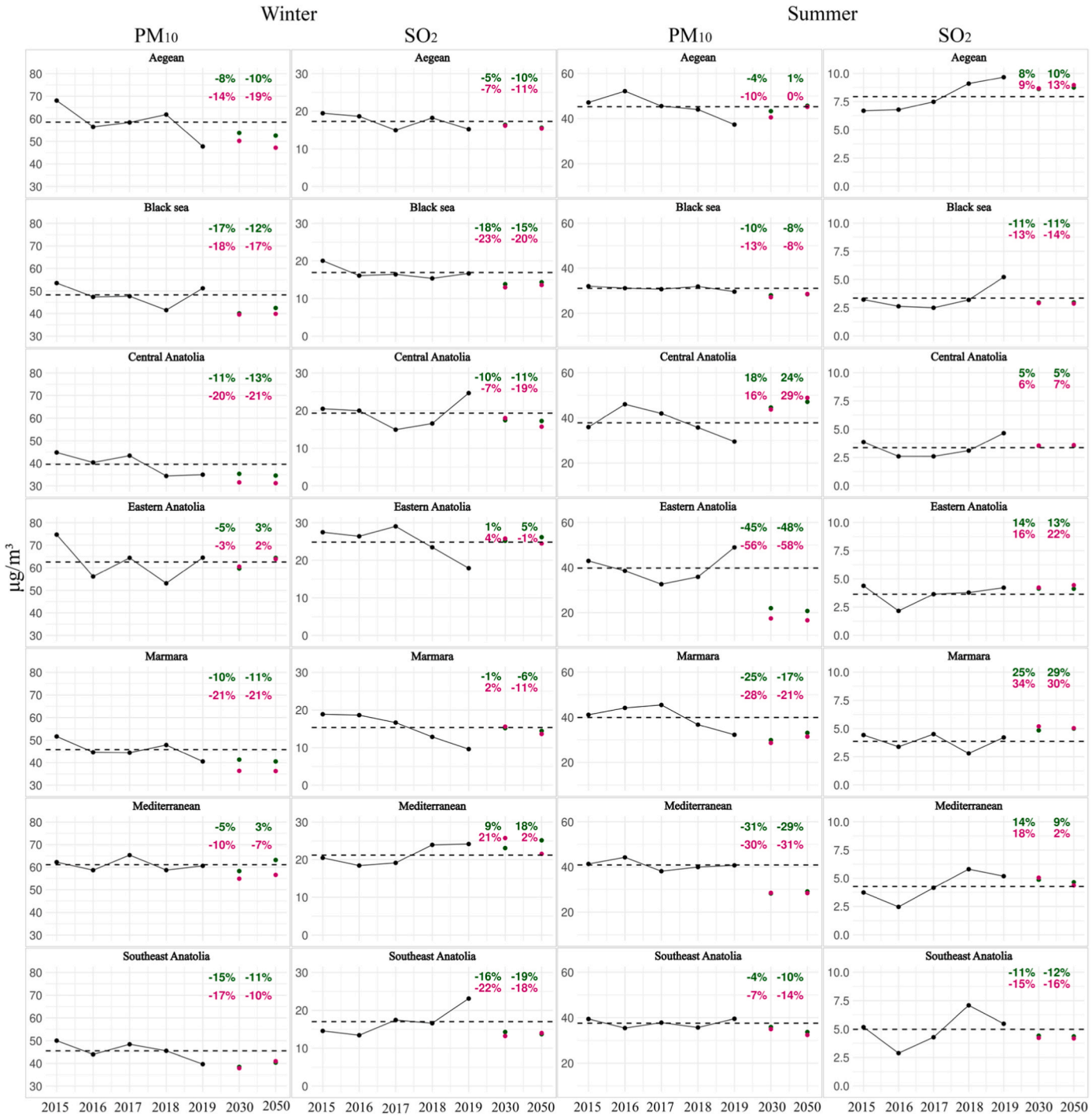

Fig. 8. Projected yearly averages of PM_{10} and SO_2 concentrations by region and season for 2030 and 2050 under RCP 4.5 (green) and RCP 8.5 (fuchsia) scenarios. Predictions are based on the generalised additive model.

direct physical effects but also indirect pathways through altered emissions patterns, chemical reaction rates, and boundary layer dynamics.

3.4. Future scenarios

This section evaluates future climatic conditions under two contrasting climate scenarios to assess their potential impact on PM_{10} and SO_2 concentrations in Türkiye for the years 2030 and 2050. The analysis focuses on the sensitivity of air quality to climate change, holding all other conditions constant. The climate scenarios are based on the IPCC Representative Concentration Pathways (RCPs): RCP 4.5 and RCP 8.5, which represent moderate and high greenhouse gas emissions pathways with different levels of mitigation efforts, respectively (CMCC, 2025).

1. RCP 4.5 (Strong Mitigation Scenario): This low emissions scenario, often referred to as "Strong Mitigation," assumes the implementation of stringent measures to control GHG emissions. It represents a stabilisation pathway, where emissions peak mid-century and subsequently decline, leading to stabilised atmospheric GHG concentrations by the end of the century. Under this scenario, global temperatures are expected to rise at a slower pace, with a reduced intensity and frequency of extreme weather events.
2. RCP 8.5 (Extreme Climate Change Scenario): The high emissions scenario, commonly associated with the term "Business-as-usual" or "No Mitigation," assumes a continued growth in GHG emissions at current rates. This scenario leads to significant global warming, characterised by more frequent and severe heatwaves, altered precipitation patterns, and changes in atmospheric pressure.

The GAM analysis of the period 2015–2019 is used to estimate the effects of changes in temperature, relative humidity, wind speed, and precipitation on pollutant concentrations in 2030 and 2050 according to the mentioned climate scenarios. The results are shown in Fig. 8, with yearly averages of PM_{10} and SO_2 concentrations by region and season. These visual representations highlight the regional variations in pollutant levels, showing the potential shifts in air pollution under both RCP 4.5 and RCP 8.5 scenarios due to the influence of atmospheric variables.

Winter projections generally indicate a potential decline in PM_{10} concentrations across all climatic regions and scenarios for both 2030 and 2050 compared to the 2015–2019 annual averages (hereafter: this is the reference period used to assess future changes). However, two exceptions emerge: in Eastern Anatolia concentrations are projected to decrease under both scenarios in 2030 but potentially increase in 2050, while in the Mediterranean region PM_{10} levels are forecasted to decline in 2030 and may rise by 2050 under RCP 4.5, whereas the model suggests they would continue to decrease under RCP 8.5 in both years. Among all the seven climatic regions, Eastern Anatolia is projected to exhibit the smallest change in PM_{10} concentrations relative to the reference period, while Central Anatolia is forecasted to show the most significant deviation. Specifically, in Central Anatolia under RCP 4.5, concentrations are projected to decrease by approximately 11 % in 2030 and 13 % in 2050, while under RCP 8.5, the model suggests reductions could reach 20 % and 21 %, respectively. In summer, both scenarios predict a general decrease in PM_{10} concentrations across all regions, with the exception of Central Anatolia where an increase is projected, with concentrations potentially rising by 18 % in 2030 and 24 % in 2050 under RCP 4.5, and by 16 % and 29 % under RCP 8.5. In the same season, Eastern Anatolia is projected to see the most pronounced decline, with potential reductions of 45 % in 2030 and 48 % in 2050 under RCP 4.5, and potentially even sharper decreases of approximately 56 % and 58 % under RCP 8.5. These model outputs suggest that seasonal differences could be significant in future projections, with summer months appearing to show more pronounced variations compared to winter.

SO_2 concentrations are projected to generally increase across most regions in summer, with the exception of the Black Sea and Southeast Anatolia, where levels are forecasted to decrease. The projected reduction in Southeast Anatolia might be associated with its high summer temperatures, which could potentially relate to increased photochemical reactions that convert SO_2 into other compounds, such as sulphate aerosols, corresponding with lower concentrations in projections (Eatough et al., 1994). In the Black Sea region, persistent year-round precipitation likely contributes to SO_2 removal through wet deposition, possibly contributing to its projected lower levels. Among all regions, Marmara is projected to have the most pronounced increase relative to the baseline, with SO_2 concentrations rising by 25 % in 2030 and 29 % in 2050 under RCP 4.5, and by 34 % in 2030 and 30 % in 2050 under RCP 8.5. Conversely, SO_2 concentrations during winter are generally projected to decrease compared to the 2015–2019 average, though some exceptions emerge. Notably, the Mediterranean region is forecasted to show an increase in SO_2 concentrations compared to the reference period: a potential rise of 9 % in 2030 and 18 % in 2050 under RCP 4.5, and 21 % in 2030 and 2 % in 2050 under RCP 8.5. This represents what appears to be the most notable difference between the two years within the same scenario across all seven regions in the projections.

These findings emphasise the critical role that future climate conditions may play in shaping air quality across Türkiye, under the assumption that emissions evolve according to the pathways defined by the selected RCP scenarios, without incorporating additional changes or external sources beyond those already considered. The results show significant variations across regions and scenarios, with notable differences between pollutants and seasons. PM_{10} concentrations are generally projected to decrease compared to the 2015–2019 average, suggesting that, if the emission trajectories and contributing factors remain as specified in the climatic scenarios, particulate matter may become a less pressing concern in many areas.

The model's outcomes show that the more extreme climate scenario (RCP 8.5) is often associated with greater reductions in PM_{10} concentrations compared to RCP 4.5 across all regions and seasons. This trend may be attributed to climate-driven changes such as higher boundary layer heights, increased wind speeds, and more frequent or intense precipitation events, all of which can enhance pollutant dispersion and removal. Additionally, warmer temperatures projected under future scenarios, particularly under RCP 8.5, may reduce the demand for residential heating in winter, leading to lower local emissions. However, the reductions presented here are based on the assumption that emissions follow the RCP scenario pathways without any unforeseen alterations. While climate conditions under RCP 8.5 may favour lower PM_{10} concentrations in some cases, the broader consequences of this high-emission scenario (such as more severe climate impacts) should not be overlooked. In contrast, SO_2 concentrations are projected to rise across nearly all regions in summer and decrease in winter in most regions (though not all). Unlike PM_{10}, SO_2 is closely tied to fixed emission sources such as industrial activities and power generation, and it appears less influenced by meteorological variables that promote dispersion.

3.4.1. Uncertainties in climate projections

Air pollution projections based on climate models are characterised by multiple sources of uncertainty that require careful consideration when interpreting results. Climate model uncertainty stems from the intrinsic variability among different global (GCM) and regional (RCM) models, each with their own parameterisations and representations of physical processes. Closely related is the downscaling uncertainty, as the reduction of scale from global to regional projections often involves simplifications and approximations that affect the accuracy of results at the local scale. In recent years, climate model experiments have increasingly aimed to support local and regional adaptation to the expected impacts of anthropogenic climate change, thereby magnifying

the role of downscaling. While downscaling enables finer-scale analysis, it introduces an additional source of uncertainty. For example, a study in the southeastern United States found that downscaling accounted for approximately 20 % of the total uncertainty in precipitation projections and around 30 % for extreme heat days (>35 °C), depending on the completeness of the downscaled ensemble used (Wootten et al., 2017).

Emission scenarios constitute a major source of uncertainty, as projections can differ markedly when additional pathways beyond the two RCPs considered in this study are included. For example, Zhu et al. (2019) found that differences between RCPs accounted for up to 50 % of the total uncertainty in runoff projections during certain months, while contributing less than 30 % in most others. This highlights the seasonal variability of scenario-related uncertainty and its frequent interplay with model-related uncertainty. Moreover, the inherent variability of the climate system (especially at decadal scales) can mask or amplify anthropogenic signals, further complicating the detection of significant trends.

All the above mentioned factors suggest that the results of our projections should be interpreted as indications of possible future trends rather than precise forecasts, highlighting the importance of developing multi-model methods and probabilistic approaches to better quantify uncertainty in future research on air quality in a changing climate.

4. Conclusions

This study contributes to the understanding of statistical relationships between atmospheric conditions and air pollution in Türkiye, by investigating the relationship between atmospheric variables and PM_{10} and SO_2 concentrations for the 2015–2019 period. It examines how variables such as temperature, humidity, wind speed, precipitation, and BLH can influence air quality across regions and seasons, using a GAM with sensitivity analysis. Projections for 2030 and 2050 under two climate scenarios—one with strong mitigation efforts and one with extreme GHG emissions—are also presented.

The relationships identified through GAM analysis reveal significant correlational patterns, but these do not necessarily imply direct causal relationships. These statistical relationships reflect fundamental physical processes governing air pollutants, such as vertical mixing, horizontal transport, and removal mechanisms, which interact to produce the complex patterns observed in the data.

The GAM outputs reveal that in winter PM_{10} levels exhibit mixed behaviour, typically peaking around 10 °C, with thermal inversions being associated with increased pollutant accumulation—particularly in the Black Sea, Eastern Anatolia, and Southeast Anatolia regions. In summer, PM_{10} shows weak positive temperature dependence, while SO_2 is negatively associated with temperature in both seasons. Relative humidity correlates positively with PM_{10} in most regions, while SO_2 generally decreases with higher humidity, especially in colder months. Higher wind speed is associated to lower PM_{10} and SO_2 levels, especially along coastal areas, with PM_{10} more responsive to wind-driven dispersion than SO_2. Precipitation is generally associated with reduced PM_{10} levels, especially in winter, while its association with SO_2 remains surprisingly weak.

The projected changes in PM_{10} and SO_2 concentrations associated with atmospheric variables under RCP 4.5 and RCP 8.5 scenarios underscore the importance of adapting air quality strategies to regional and seasonal variations. While meteorological conditions are generally linked to reductions in PM_{10} levels across most areas and both seasons, their relationship with SO_2 suggests potential increases during summer, highlighting the need for targeted mitigation measures.

While this study provides valuable insights, some limitations should be acknowledged. A significant limitation is that the study relies on surface meteorological measurements to draw inferences about complex vertical atmospheric processes. Without direct measurements of vertical temperature profiles, our interpretations regarding thermal inversions and boundary layer dynamics remain speculative. Additionally, there is a lack of validation against process-based atmospheric models, such as WRF-Chem or CMAQ, which explicitly represent atmospheric dynamics. To address these methodological limitations, future research should: (1) incorporate radiosonde data, lidar measurements, or other vertical profiling techniques; and (2) compare statistical findings with mechanistic approaches to evaluate consistency. Additionally, future research in Türkiye should adopt quasi-experimental designs or analyses of policy interventions to better isolate causal relationships between atmospheric variables and air pollution. The integration of longer-term studies, high-resolution satellite data, and the extension of the analysis to additional pollutants and seasonal periods would allow for a deeper understanding of pollutant variability and its determinants. Additionally, pollutant concentrations are also influenced by several factors not addressed in this study, such as variations in emission sources (patterns in traffic and industrial activity), changes in energy consumption behaviour, agricultural activities, and episodic events (i.e. wildfires, dust storms). Transboundary pollution transport also remains an important external contributor. To better understand source attribution, enhanced models that incorporate emission inventories, land-use data, and sector-specific activity patterns are essential (Belis et al., 2020, 2021).

The results of this study suggest that national air quality strategies may not be universally effective, emphasising the need for region-specific mitigation efforts—particularly in areas where both PM_{10} and SO_2 levels are projected to rise.

Meteorologically driven pollution dynamics can significantly influence economic policy decisions by enabling more cost-effective and targeted regulatory strategies. For instance, the OECD employs thermal inversions as an instrumental variable in a two-stage estimation approach, first using weather patterns to predict pollution, then linking it to economic outcomes (Dechezleprêtre et al., 2019)—showing how climate signals can be translated into actionable policy levers. In Türkiye, where evidence-based policymaking is urgent given current climate and air-quality governance gaps (European Commission, 2024), including persistent coal-based emissions, limited alignment with EU standards, and the absence of a long-term emission-reduction strategy, this study's findings are especially relevant. The results provide a practical basis to implement or update policies already in force, including meteorology-based episode plans and tighter fuel-quality and stack-emission enforcement under Environment Law No. 2872 (2022). They also supply an evidence base for voluntary alignment with the UNECE Gothenburg Protocol framework—Türkiye has not signed or ratified—by prioritising emission-ceiling-style measures, thereby advancing convergence with the EU air-quality acquis and helping policymakers target resources for measurable health gains at lower cost. In this context, the insights offered by this study provide a practical foundation for strengthening environmental governance and guiding more targeted, forward-looking policy action for sustainable development and improved public well-being.

CRediT authorship contribution statement

Sara Ciarlantini: Writing – original draft, Visualization, Methodology, Formal analysis, Data curation. **Claudio A. Belis:** Writing – review & editing, Supervision, Conceptualization. **Andreas Gavros:** Visualization, Data curation. **Alessandro Pezzoli:** Writing – review & editing, Supervision, Conceptualization, Validation.

Funding source

This research did not receive any specific grant from funding agencies in the public, commercial, or not-for-profit sectors.

Declaration of competing interest

The authors declare that they have no known competing financial interests or personal relationships that could have appeared to influence

the work reported in this paper.

Acknowledgements

The authors express their sincere gratitude to Lorenzo Minola for his valuable contribution to this work, particularly for downloading the ERA5 datasets, and especially for his insightful suggestions, careful reading, and constructive revisions of the manuscript. They also thank Eugenio Merlo, a master's student at the University of Turin, for his support during the initial data download and preliminary analysis, carried out as part of his master degree's final dissertation.

Appendix A. Supplementary data

Supplementary data to this article can be found online at https://doi.org/10.1016/j.apr.2025.102826.

References

Akaike, H., 1974. A new look at the statistical model identification. IEEE Trans. Autom. Control 19 (6).

Alwateer, M., Atlam, E.-S., El-Raouf, M.M.A., Ghoneim, O.A., Gad, I., 2024. Missing data imputation: a comprehensive review. JCC 12, 53–75. https://doi.org/10.4236/jcc.2024.1211004.

Aykaç, N., Yasin, Y., 2021. Persistent ambient air pollution in Turkey: a 4-year analysis. Turk Thorac J 22, 482–488. https://doi.org/10.5152/TurkThoracJ.2021.21121.

Belis, C.A., Pernigotti, D., Pirovano, G., Favez, O., Jaffrezo, J.L., Kuenen, J., Denier Van Der Gon, H., Reizer, M., Riffault, V., Alleman, L.Y., Almeida, M., Amato, F., Angyal, A., Argyropoulos, G., Bande, S., Beslic, I., Besombes, J.-L., Bove, M.C., Brotto, P., Calori, G., Cesari, D., Colombi, C., Contini, D., De Gennaro, G., Di Gilio, A., Diapouli, E., El Haddad, I., Elbern, H., Eleftheriadis, K., Ferreira, J., Vivanco, M.G., Gilardoni, S., Golly, B., Hellebust, S., Hopke, P.K., Izadmanesh, Y., Jorquera, H., Krajsek, K., Kranenburg, R., Lazzeri, P., Lenartz, F., Lucarelli, F., Maciejewska, K., Manders, A., Manousakas, M., Masiol, M., Mircea, M., Mooibroek, D., Nava, S., Oliveira, D., Paglione, M., Pandolfi, M., Perrone, M., Petralia, E., Pietrodangelo, A., Pillon, S., Pokorna, P., Prati, P., Salameh, D., Samara, C., Samek, L., Saraga, D., Sauvage, S., Schaap, M., Scotto, F., Sega, K., Siour, G., Tauler, R., Valli, G., Vecchi, R., Venturini, E., Vestenius, M., Waked, A., Yubero, E., 2020. Evaluation of receptor and chemical transport models for PM10 source apportionment. Atmos. Environ. X 5, 100053. https://doi.org/10.1016/j.aeaoa.2019.100053.

Belis, C.A., Pirovano, G., Villani, M.G., Calori, G., Pepe, N., Putaud, J.P., 2021. Comparison of source apportionment approaches and analysis of non-linearity in a real case model application. Geosci. Model Dev. (GMD) 14, 4731–4750. https://doi.org/10.5194/gmd-14-4731-2021.

Berger, V.W., Zhou, Y., 2014. Kolmogorov–Smirnov Test: Overview. Wiley StatsRef: Statistics Reference Online, John Wiley & Sons, Ltd. https://doi.org/10.1002/9781118445112.stat06558.

Bozkurt, Z., Üzmez, Ö.Ö., Döğeroğlu, T., Artun, G., Gaga, E.O., 2018. Atmospheric concentrations of SO2, NO2, ozone and VOCs in Düzce, Turkey using passive air samplers: sources, spatial and seasonal variations and health risk estimation. Atmos. Pollut. Res. 9, 1146–1156. https://doi.org/10.1016/j.apr.2018.05.001.

Çapraz, Ö., Efe, B., Deniz, A., 2016. Study on the association between air pollution and mortality in Istanbul, 2007-2012. Atmos. Pollut. Res. https://doi.org/10.1016/j.apr.2015.08.006.

Çelik, M.B., Kadi, I., 2007. The relation between meteorological factors and pollutants concentrations in Karabük city, G.U. J. Sci. 20, 87–95.

Chai, T., Draxler, R.R., 2014. Root mean square error (RMSE) or mean absolute error (MAE)? – arguments against avoiding RMSE in the literature. Geosci. Model Dev. 7, 1247–1250. https://doi.org/10.5194/gmd-7-1247-2014.

CMCC, 2025. Scenari climatici per l'Italia. https://www.cmcc.it/it/scenari-climatici-per-litalia. (Accessed 17 March 2025).

Colston, J.M., Ahmed, T., Mahopo, C., Kang, G., Kosek, M., De Sousa Junior, F., Shrestha, P.S., Svensen, E., Turab, A., Zaitchik, B., 2018. Evaluating meteorological data from weather stations, and from satellites and global models for a multi-site epidemiological study. Environ. Res. 165, 91–109. https://doi.org/10.1016/j.envres.2018.02.027.

Copernicus, 2024. Climate data Store. https://cds.climate.copernicus.eu/datasets?q=projections. (Accessed 28 February 2025).

Cuhadaroglu, B., Demirci, E., 1997. Influence of some meteorological factors on air pollution in Trabzon city. Energy Build. 25, 179–184. https://doi.org/10.1016/S0378-7788(96)00992-9.

Dechezleprêtre, A., Rivers, N., Stadler, B., 2019. The Economic Cost of Air Pollution: Evidence from Europe Economics Department Working Papers No. 1584. OECD.

DEFRA, UK Air, 2023. Site environment types. https://uk-air.defra.gov.uk/networks/site-types. (Accessed 13 November 2024).

Demir, M., Dindaroğlu, T., Yılmaz, S., 2014. Effects of forest areas on air quality; Aras Basin and its environment. J. Environ. Health Sci. Eng. 12, 60. https://doi.org/10.1186/2052-336X-12-60.

Deniz, A., Toros, H., Incecik, S., 2011. Spatial variations of climate indices in Turkey. Intl Journal of Climatology 31, 394–403. https://doi.org/10.1002/joc.2081.

Donders, A.R.T., van der Heijden, G.J.M.G., Stijnen, T., Moons, K.G.M., 2006. Review: a gentle introduction to imputation of missing values. J. Clin. Epidemiol. 59, 1087–1091. https://doi.org/10.1016/j.jclinepi.2006.01.014.

Eatough, D.J., Caka, F.M., Farber, R.J., 1994. The conversion of SO_2 to sulfate in the atmosphere. Isr. J. Chem. 34, 301–314. https://doi.org/10.1002/ijch.199400034.

ECMWF, 2024. Climate data Store. https://cds.climate.copernicus.eu/. (Accessed 13 November 2024).

EEA, 2023. Europe's air quality status. https://www.eea.europa.eu/publications/europes-air-quality-status-2023/europes-air-quality-status2023. (Accessed 22 August 2024), 2023.

EEA, 2024. https://www.eea.europa.eu/en. (Accessed 13 November 2024).

EEA, 2025. Nitrogen dioxide - no2. https://www.eea.europa.eu/en/analysis/publications/air-quality-status-report-2025/nitrogen-dioxide. (Accessed 11 November 2024).

Environment Law No. 2872, 2022. https://www.ecolex.org/details/legislation/environment-law-no-2872-lex-faoc007700/. (Accessed 24 October 2025) last access.

EPA, 2024. Sulfur dioxide basics. https://www.epa.gov/so2-pollution/sulfur-dioxide-basics. (Accessed 12 November 2024).

European Commission, 2023. Türkiye 2023 Report Accompanying the Document Communication from the Commission to the European Parliament, the Council, the European Economic and Social Committee and the Committee of the Regions. 2023 Communication on EU Enlargement Policy, 696 final. Brussels 2023.

European Commission, 2024. Commission Staff Working Document - Türkiye 2024 Report, vol. 696. Brussels.

European Parliament and Council, 2024. Directive (EU) 2024/2881 on ambient air quality and cleaner air for Europe. Off. J. Eur. Union.

FAO, 2024. FAO in Türkiye. Türkiye at a glance: https://www.fao.org/turkiye/fao-in-turkiye/turkey-at-a-glance/en/. (Accessed 13 November 2024).

Feng, X., Wei, S., Wang, S., 2020. Temperature inversions in the atmospheric boundary layer and lower troposphere over the Sichuan Basin, China: climatology and impacts on air pollution. Sci. Total Environ. 726, 138579. https://doi.org/10.1016/j.scitotenv.2020.138579.

Güneş, M., 2005. A simple evaluation of SO2 and PM data on ambient air quality. Energy Sources 27, 729–740. https://doi.org/10.1080/00908310490450449.

Han, L., Zhou, W., Li, W., Meshesha, D.T., Li, L., Zheng, M., 2015. Meteorological and urban landscape factors on severe air pollution in Beijing. J. Air Waste Manag. Assoc. 65, 782–787. https://doi.org/10.1080/10962247.2015.1007220.

Hastie, T.J., 2017. Generalized Additive Models. Routledge, New York. https://doi.org/10.1201/9780203753781.

HEI, 2025. State of Global Air 2025: a Report on Air Pollution and its Role in the World's Leading Causes of Death. Health Effects Institute, Boston, MA.

Hersbach, H., Bell, B., Berrisford, P., Hirahara, S., Horányi, A., Muñoz-Sabater, J., Nicolas, J., et al., 2020. The ERA5 global reanalysis. Q. J. R. Meteorol. Soc. 146, 1999–2049. https://doi.org/10.1002/qj.3803.

Hou, K., Xu, X., 2022. Evaluation of the influence between local meteorology and air quality in Beijing using generalized additive models. Atmosphere 13, 24. https://doi.org/10.3390/atmos13010024.

İçağa, Y., Sabah, E., 2009. Statistical analysis of air pollutants and meteorological parameters in Afyon, Turkey. Environ. Model. Assess. 14, 259–266. https://doi.org/10.1007/s10666-008-9139-5.

IHME - GHDx, 2019. GBD results. https://vizhub.healthdata.org/gbd-results. (Accessed 22 January 2024).

IQAir, 2024. World air quality report. Region & City PM2.5 Ranking.

Kabatas, B., Unal, A., Pierce, R.B., Kindap, T., Pozzoli, L., 2014. The contribution of Saharan dust in PM10 concentration levels in Anatolian Peninsula of Turkey. Sci. Total Environ. 488–489, 413–421. https://doi.org/10.1016/j.scitotenv.2013.12.045.

Joint Research Centre, 2024. SIMLAB reference manual POLIS-JRC ISIS. Joint Research Centre of the European Community. https://web.jrc.ec.europa.eu/rapps/pub/simlab/.

Kabatas, B., Pierce, R.B., Unal, A., Rogal, M.J., Lenzen, A., 2018. April 2008 Saharan dust event: its contribution to PM10 concentrations over the Anatolian Peninsula and relation with synoptic conditions. Sci. Total Environ. 633, 317–328. https://doi.org/10.1016/j.scitotenv.2018.03.150.

Kartal, S., Özer, U., 1998. Determination and parameterization of some air pollutants as a function of meteorological parameters in Kayseri, Turkey. J. Air Waste Manag. Assoc. 48, 853–859. https://doi.org/10.1080/10473289.1998.10463738.

Kayes, I., Shahriar, S.A., Hasan, K., Akhter, M., Kabir, M.M., Salam, M.A., 2019. The relationships between meteorological parameters and air pollutants in an urban environment. Global J. Environ. Sci. Manage 5. https://doi.org/10.22034/GJESM.2019.03.01.

Latini, G., Grifoni, R.C., Passerini, G., 2002. Influence of meteorological parameters on urban and suburban air pollution. Air Pollution X.

Ledoux, F., Roche, C., Delmaire, G., Roussel, G., Favez, O., Fadel, M., Courcot, D., 2023. Measurement report: a 1-year study to estimate maritime contributions to PM_{10} in a coastal area in northern France. Atmos. Chem. Phys. 23, 8607–8622. https://doi.org/10.5194/acp-23-8607-2023.

Lenschow, P., 2001. Some ideas about the sources of PM10. Atmos. Environ. 35, 23–33. https://doi.org/10.1016/S1352-2310(01)00122-4.

Little, R.J.A., 1988. A test of missing completely at random for multivariate data with missing values. J. Am. Stat. Assoc. 83, 1198–1202. https://doi.org/10.1080/01621459.1988.10478722.

Ma, S., Shao, M., Zhang, Y., Dai, Q., Xie, M., 2021. Sensitivity of PM2.5 and O3 pollution episodes to meteorological factors over the North China Plain. Sci. Total Environ. 792, 148474. https://doi.org/10.1016/j.scitotenv.2021.148474.

MacFarland, T.W., Yates, J.M., 2016. Mann–Whitney U Test, Introduction to Nonparametric Statistics for the Biological Sciences Using R. Springer, Cham, pp. 103–132. https://doi.org/10.1007/978-3-319-30634-6_4.

Manju, A., Kalaiselvi, K., Dhananjayan, V., Palanivel, M., Banupriya, G.S., Vidhya, M.H., Panjakumar, K., Ravichandran, B., 2018. Spatio-seasonal variation in ambient air pollutants and influence of meteorological factors in Coimbatore, Southern India. Air Qual. Atmos. Health 11, 1179–1189. https://doi.org/10.1007/s11869-018-0617-x.

McKight, P.E., Najab, J., 2010. Kruskal-Wallis Test, the Corsini Encyclopedia of Psychology. John Wiley & Sons, Ltd. https://doi.org/10.1002/9780470479216.corpsy0491.

NOAA, 2024. National Centers for Environmental Information (NCEI). https://www.ncei.noaa.gov/. (Accessed 13 November 2024).

Pearce, J.L., Beringer, J., Nicholls, N., Hyndman, R.J., Tapper, N.J., 2011. Quantifying the influence of local meteorology on air quality using generalized additive models. Atmos. Environ. 45, 1328–1336. https://doi.org/10.1016/j.atmosenv.2010.11.051.

Pianosi, F., Wagener, T., 2015. A simple and efficient method for global sensitivity analysis based on cumulative distribution functions. Environ. Model. Software 67, 1–11. https://doi.org/10.1016/j.envsoft.2015.01.004.

Plischke, E., Borgonovo, E., Smith, C.L., 2013. Global sensitivity measures from given data. Eur. J. Oper. Res. 226, 536–550. https://doi.org/10.1016/j.ejor.2012.11.047.

Qi, X., Mei, G., Cuomo, S., Liu, C., Xu, N., 2021. Data analysis and mining of the correlations between meteorological conditions and air quality: a case study in Beijing. Internet of Things 14, 100127. https://doi.org/10.1016/j.iot.2019.100127.

Ravindra, K., Rattan, P., Mor, S., Aggarwal, A.N., 2019. Generalized additive models: building evidence of air pollution, climate change and human health. Environ. Int. 132, 104987. https://doi.org/10.1016/j.envint.2019.104987.

Sahin, S., Kerem Cigizoglu, H., 2012. The sub-climate regions and the sub-precipitation regime regions in Turkey. J. Hydrol. 450–451, 180–189. https://doi.org/10.1016/j.jhydrol.2012.04.062.

Sahin, S., Türkeş, M., 2013. Contemporary surface wind climatology of Turkey. Theor. Appl. Climatol. 113, 337–349. https://doi.org/10.1007/s00704-012-0789-5.

Şahin, S., Türkeş, M., 2020. Assessing wind energy potential of Turkey via vectoral map of prevailing wind and mean wind of Turkey. Theor. Appl. Climatol. 141, 1351–1366. https://doi.org/10.1007/s00704-020-03276-3.

Sensoy, S., Demircan, M., 2016. Climate of Turkey.

Tasdemir, Y., Cindoruk, S.S., Esen, F., 2005. Monitoring of criteria air pollutants in Bursa, Turkey. Environ. Monit. Assess. 110, 227–241. https://doi.org/10.1007/s10661-005-7866-5.

Tayanç, M., Karaca, M., Yenigün, O., 1997. Annual and seasonal air temperature trend patterns of climate change and urbanization effects in relation to air pollutants in Turkey. J. Geophys. Res. 102, 1909–1919. https://doi.org/10.1029/96JD02108.

Thompson, M., 2001. A review of statistical methods for the meteorological adjustment of tropospheric ozone. Atmos. Environ. 35, 617–630. https://doi.org/10.1016/S1352-2310(00)00261-2.

THPP. Right to Clean Air Platform, 2024. Air pollution and health impacts. Dark Report 2024. https://temizhavahakki.org/en/dark-report-2024/.

Türkeş, M., 1996. Spatial and temporal analysis of annual rainfall variations in Turkey. Int. J. Climatol. 16, 1057–1076. https://doi.org/10.1002/(SICI)1097-0088(199609)16:9<1057::AID-JOC75>3.0.CO;2-D.

Ulutaş, K., Abujayyab, S.K.M., Abu Amr, S., 2021. Evaluation of the major air pollutants levels and its interactions with meteorological parameters in Ankara. Mühendislik Bilimleri ve Tasarım Dergisi 9, 1284–1295. https://doi.org/10.21923/jesd.939724.

UNEP, 2023. World must band together to combat air pollution. which kills 7 million a year. https://www.unep.org/news-and-stories/story/world-must-band-together-combat-air-pollution-which-kills-7-million-year. (Accessed 10 January 2024).

Van Nieuwenhuyse, J., Van Schaeybroeck, B., Caluwaerts, S., De Deyn, J., Delcloo, A., De Troch, R., Hamdi, R., Termonia, P., 2023. Air-stagnation episodes based on regional climate models part I: evaluation over Europe. Clim. Dyn. 61, 2121–2138. https://doi.org/10.1007/s00382-023-06665-2.

WHO, 2024. Ambient (outdoor) air pollution. https://www.who.int/news-room/fact-sheets/detail/ambient-(outdoor)-air-quality-and-health. (Accessed 26 October 2024).

WHO, 2021. WHO global air quality guidelinesParticulate Matter (PM2.5 and PM10), Ozone, Nitrogen Dioxide, Sulfur Dioxide and Carbon Monoxide. Geneva.

WMO, 2017. WMO Guidelines on the Calculation of Climate Normals (WMO-No. 1203). Geneva.

Wootten, A., Terando, A., Reich, B.J., Boyles, R.P., Semazzi, F., 2017. Characterizing sources of uncertainty from global climate models and downscaling techniques. J. Appl. Meteorol. Climatol. 56 (12), 3245–3262. https://doi.org/10.1175/JAMC-D-17-00871.

World Bank, 2022. The global health cost of PM2.5 air pollution: a case for action beyond 2021. International Development in Focus. World Bank, Washington, DC. https://doi.org/10.1596/978-1-4648-1816-5. License: Creative Commons Attribution CC BY 3.0 IGO.

Yan, H., Li, Q., Feng, K., Zhang, L., 2023. The characteristics of PM emissions from construction sites during the earthwork and foundation stages: an empirical study evidence. Environ. Sci. Pollut. Res. 30, 62716–62732. https://doi.org/10.1007/s11356-023-26494-4.

Zhu, X., Zhang, A., Wu, P., Qi, W., Fu, G., Yue, G., Liu, X., 2019. Uncertainty impacts of climate change and downscaling methods on future runoff projections in the biliu River Basin. Water 11, 2130. https://doi.org/10.3390/w11102130.

Zuur, A.F., 2012. A Beginner's Guide to Generalized Additive Models with R. Highland Statistics Ltd, Newburgh, United Kingdom.